Chemistry & Biology
Article

Affinity Reagents that Target a Specific Inactive Form of Protein Kinases

Pratistha Ranjitkar,[1] Amanda M. Brock,[1] and Dustin J. Maly[1,*]
[1]Department of Chemistry, University of Washington, Seattle, WA 98195, USA
*Correspondence: maly@chem.washington.edu
DOI 10.1016/j.chembiol.2010.01.008

SUMMARY

A number of small-molecule inhibitors have been developed that target the catalytic domains of protein kinases that are not in an active conformation. An inactive form that has been observed in several kinases is the DFG-out conformation. This conformation is characterized by an almost 180° rotation of the conserved Asp-Phe-Gly (DFG) motif in the ATP-binding cleft relative to the active form. However, the sequence and structural determinants that allow a kinase to stably adopt the DFG-out conformation are not known. Here, we characterize a series of inhibitors based on a general pharmacophore for this inactive form. We demonstrate that modified versions of these inhibitors can be used to study the thermodynamics and kinetics of ligand binding to DFG-out-adopting kinases and for enriching these kinases from complex protein mixtures.

INTRODUCTION

Comprised of over 500 members, protein kinases are the largest enzyme family encoded by the human genome (Manning et al., 2002). These enzymes are the major mediators of intracellular protein phosphorylation cascades and are involved in complex phenotypic responses such as growth, differentiation, adhesion, and motility (Cohen, 2000). The proper spatial and temporal control of intracellular phosphorylation events by protein kinases is essential for normal cellular function. Indeed, aberrant kinase activity has been implicated in numerous diseases including cancer, diabetes, and chronic inflammation (Cohen, 2002). For this reason, there has been considerable effort toward the development of pharmacological agents that target this enzyme family.

The overall structure of the catalytic domain of protein kinases is highly conserved (Figure 1A) (Hanks and Hunter, 1995). It consists of 250–300 residues that form a bi-lobal structure containing a smaller, mostly β stranded, N-terminal domain and a larger, mostly α-helical, C-terminal domain (Taylor et al., 1988). Adenosine 5′-triphosphate (ATP) sits in a narrow hydrophobic cleft between the N- and C-terminal lobes, with the purine moiety forming a pair of hydrogen bonds with the hinge region (Engh and Bossemeyer, 2001). Most protein kinases possess at least two distinct catalytic states: an active state where all of the catalytic residues are in an optimal position for phosphate transfer and an inactive state (or states) with reduced catalytic activity (Huse and Kuriyan, 2002). The conformation of the ATP-binding site in these two states can be quite distinct, characterized by large conformational shifts in several conserved catalytic residues. A number of phosphorylation events and protein-protein interactions regulate the conformational state of these enzymes (Jeffrey et al., 1995; Pellicena and Kuriyan, 2006; Wong et al., 2004).

The ATP-binding sites of protein kinases in the active conformation are very similar, while the structures of inactive kinases are much more varied (Engh and Bossemeyer, 2001; Kornev et al., 2006). A specific inactive form of the ATP-binding cleft that has been observed in a number of kinases is the DFG-out conformation (Liu and Gray, 2006; Okram et al., 2006). Several potent kinase inhibitors have been found to selectively bind to the DFG-out conformation of their kinase targets (type II inhibitors). In many cases, these type II inhibitors exhibit a high degree of selectivity. Despite the selectivity demonstrated by some type II inhibitors, a set of conserved binding interactions in the ATP-binding pocket has been observed (Jacobs et al., 2008; Liu and Gray, 2006; Nagar et al., 2002; Okram et al., 2006; Simard et al., 2009a). While the DFG-out conformation appears to be energetically accessible to a number of kinases, the sequence and structural determinants that allow this transition are still poorly understood. Furthermore, it is still not possible to predict which members of the kinome can be effectively targeted with type II inhibitors. Identifying the full complement of kinases that are able to stably adopt this inactive conformation will shed light on the catalytic regulation of protein kinases and may yield new targets for drug discovery.

Here we report the development of a set of affinity probes that are derived from a general type II ligand for the DFG-out conformation of protein kinases. We show that fluorophore-conjugated analogs of these ligands are useful probes for measuring the thermodynamics and kinetics of type II inhibitor binding to protein kinases. In addition, we demonstrate that these reagents are capable of selectively enriching protein kinases that can adopt this inactive form from complex protein mixtures. Using these probes we provide evidence that the STE20 kinase LOK behaves like a kinase that can adopt the DFG-out conformation.

RESULTS

A General Type II Inhibitor Scaffold

In order to develop a set of reagents for investigating inactive forms of protein kinases we wished to identify a general ligand for the DFG-out conformation. Recently, we have characterized a series of triazolopyridines that are equipotent inhibitors of the

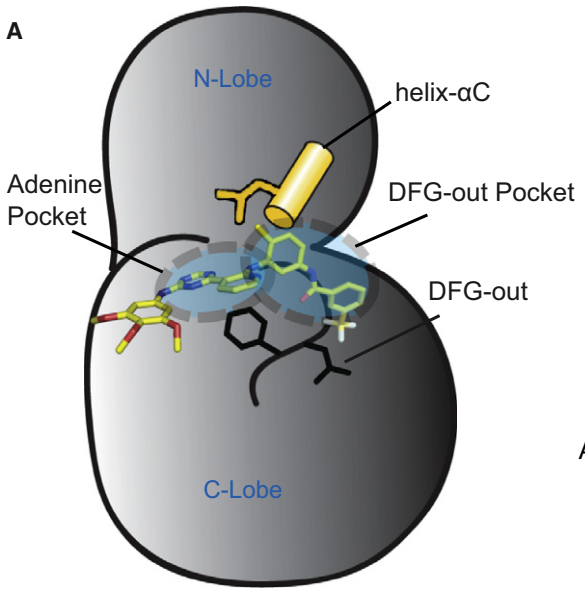

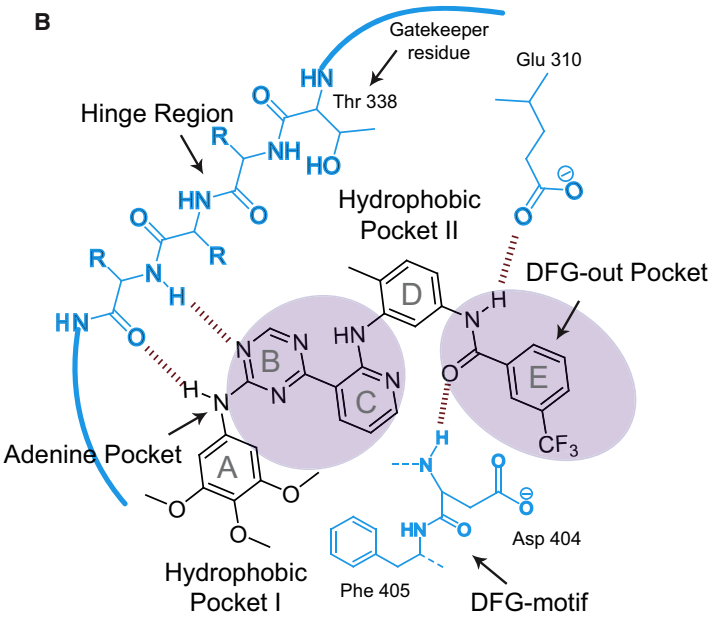

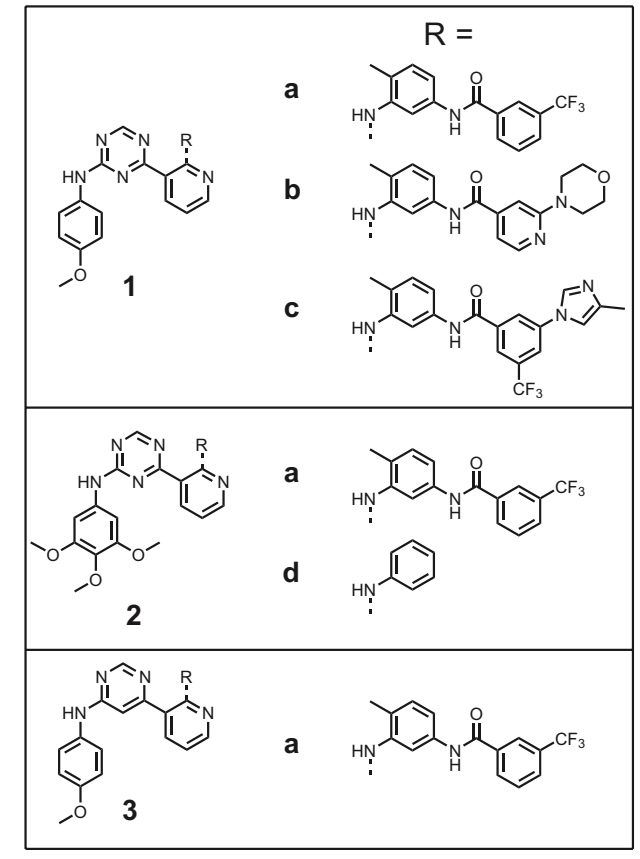

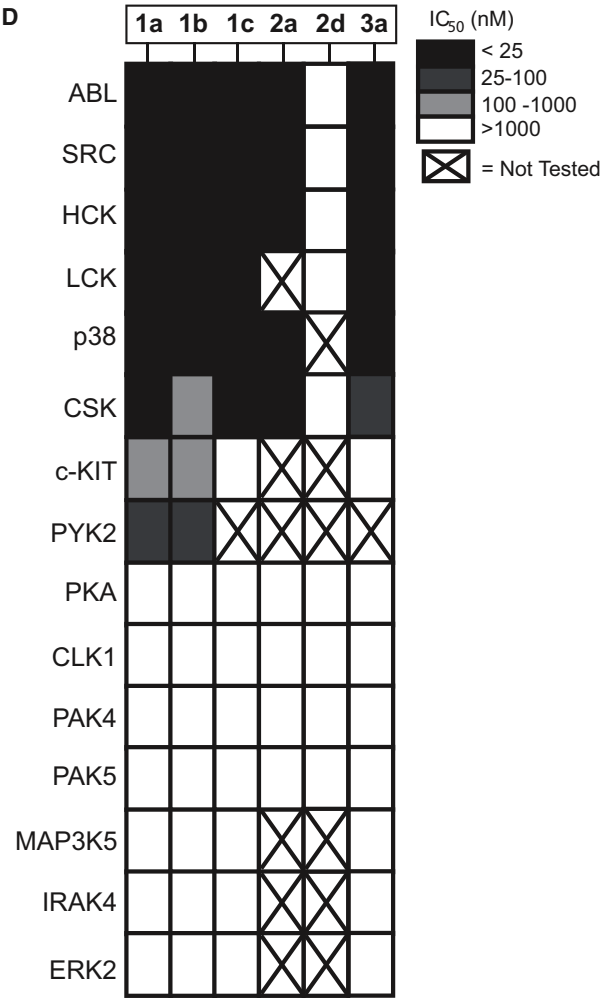

tyrosine kinases SRC and ABL (Seeliger et al., 2009). Through structural and kinetic studies we demonstrated that this class of inhibitors binds to the DFG-out conformation of these kinases. The general binding mode of the triazolopyridine ligands is similar to other type II inhibitors that have been described (Figure 1B; PDB IDs: 3G6G and 3G6H). The aniline and triazine groups (rings A and B) form a pair of hydrogen bonds with the hinge region and occupy the hydrophobic cleft used by adenine. Rings C and D serve as a linker connecting the adenine-binding region to a hydrophobic pocket (DFG-out pocket) that is created by the nearly 180° rotation of the Phe in the DFG motif to a more solvent-exposed position. Upon entering the DFG-out pocket, the amide group connecting rings D and E forms a pair of hydrogen bonds with a conserved glutamate in the helix αC and the backbone of the DFG motif. Finally, ring E occupies the DFG-out pocket. A small panel of inhibitors based on the triazolopyridine scaffold was generated to determine the generality of this ligand class (Figure 1C). For inhibitor series **1** and **2**, the substituents that occupy the DFG-out pocket and exit the adenine-binding site were varied (rings A and E), while the core scaffold (rings B, C, and D) was held constant. Compounds **1a** and **2a** contain a 3-trifluoromethylbenzamide group, which is a common binding element in many type II inhibitors (Liu and Gray, 2006; Okram et al., 2006). Compounds **1b** and **1c** contain functional groups that are components of selective type II inhibitors: **1b** contains a 2-morphilinopyridyl group, which is the pharmacophore that occupies the DFG-out pocket in the selective type II p38 MAPK inhibitor MPAQ, and compound **1c** contains the functional groups that are present in the selective type II BCR-ABL inhibitor nilotinib (Cumming et al., 2004; Sullivan et al., 2005; Weisberg et al., 2005). Finally, compound **2d** was generated as a control compound due to its lack of a substituent that occupies the DFG-out pocket. In addition to the triazolopyridine inhibitors from series **1**, a pyrimidinepyridine compound (**3a**) was also generated to determine the role of scaffold structure.

To determine whether the inhibitors generated are potent ligands for kinases that adopt the DFG-out conformation, they were tested against a panel of kinases in which high resolution crystal structures of the catalytic domain are available. Crystal structures of the tyrosine kinases SRC, LCK, ABL, PYK2, CSK, and c-KIT and the serine/threonine kinase p38α in the DFG-out conformation have been obtained and these kinases have been found to be sensitive to type II inhibitors (Han et al., 2009; Mol et al., 2004; Seeliger et al., 2009; Simard et al., 2009b). In contrast, the serine/threonine kinases PKA, PAK4, PAK5, CLK1, MAP3K5, IRAK4, and ERK2 have not been observed in this inactive form and inhibitor selectivity screens have shown them to only be sensitive to type I inhibitors (Fedorov et al., 2007). The results of the inhibition assays are shown in Figure 1D. SRC, LCK, ABL, PYK2, CSK, HCK, p38, and c-KIT were potently inhibited by most of the type II inhibitors (**1a**–**1c**, **2a**, and **3a**), while kinases that have not previously been observed in the DFG-out conformation show little or no inhibition at the highest concentration tested (1 μM). Consistent with these inhibitors binding to the DFG-out conformation, control compound **2d** shows minimal inhibition of kinases that are sensitive to type II inhibitors. Surprisingly, the identity of the aryl group that projects into the DFG-out pocket has only a small impact on the selectivity profile among DFG-out-adopting kinases.

BODIPY-Labeled Compounds as Binding Probes for Protein Kinases

In most cases, the potencies of compounds that bind the DFG-out inactive conformation have been determined by their ability to inhibit activated kinases. However, this method of analysis does not allow kinase forms with low catalytic activity to be probed and it is often difficult to correlate the observed inhibition to the binding of a specific kinase conformation. A direct binding assay has the ability to measure ligand affinity for any activation state of a protein kinase and allows binding kinetics to be determined. For this reason, we determined the feasibility of converting our general type II inhibitors into fluorescently-labeled binding probes. Based on a previously reported crystal structure of inhibitor **2a** bound to SRC, the solvent-exposed 4-position of ring A was selected as the site of fluorophore attachment (Figure 2A). Because inhibitors **1a** and **2a** have similar potencies against most kinases, a BODIPY-FL fluorophore was conjugated to the monoalkoxy derivative **1a**. To determine whether fluorophore attachment significantly affects the potency of this inhibitor against protein kinases, in vitro activity assays were performed with p38 and SRC. Gratifyingly, the IC_{50} of probe **4a** for SRC and p38 is similar to inhibitor **1a** (Figure 2B).

We hypothesized that probe **4a** would show an increase in fluorescence when bound to the ATP-binding cleft of a protein kinase. To test this, 10 nM of probe **4a** was incubated with increasing concentrations of the catalytic domains of ABL or p38 (1–250 nM). In the presence of these kinases, probe **4a** demonstrated a concentration-dependent increase in fluorescence (Figure 2C, top). To confirm that the observed increase in fluorescence is due to a specific interaction in the ATP-binding pocket, this experiment was repeated in the presence of an excess of a competitor that does not contain a fluorophore (1 μM of **1a**). As expected, no increase in fluorescence was observed for either kinase in the presence of excess competitor (Figure 2C). Having validated our binding assay with p38 and ABL, the K_d values of probe **4a** for a panel of kinases was

Figure 1. The DFG-Out Conformation of Protein Kinases and Type II Inhibitors

(A) The catalytic domain of the tyrosine kinase SRC bound to the type II inhibitor **2a**. The ATP-binding cleft is in the DFG-out conformation. The conserved glutamate in helix αC (shown in yellow) and the conserved aspartate and phenylalanine in the DFG motif (shown in black) are in conformations observed for kinases bound to type II inhibitors. Kinase subpockets occupied by type II inhibitors are indicated by dashed circles.

(B) A schematic representation of **2a** bound to the tyrosine kinase SRC. This inhibitor forms two hydrogen bonds with the hinge region of the kinase. The characteristic set of hydrogen bonds that type II inhibitors form with the conserved glutamate residue in the helix αC and the amide backbone of the aspartate of the DFG motif are shown. The DFG-out pocket that is generated by the movement of the phenylalanine residue of the DFG motif is shaded.

(C) Chemical structures of inhibitors **1a**-**1c**, **2a**, **2d**, and **3a**.

(D) IC_{50}s of the inhibitors shown in (C) against a diverse panel of kinases. Potencies are represented in grayscale. Note: We have previously reported the IC_{50}s of inhibitors **1a** and **2a** for SRC, ABL, and HCK (Seeliger et al., 2009). In this publication these compounds are referred to as **DSA7** and **DSA1**, respectively. All assays were run in triplicate or quadruplicate.

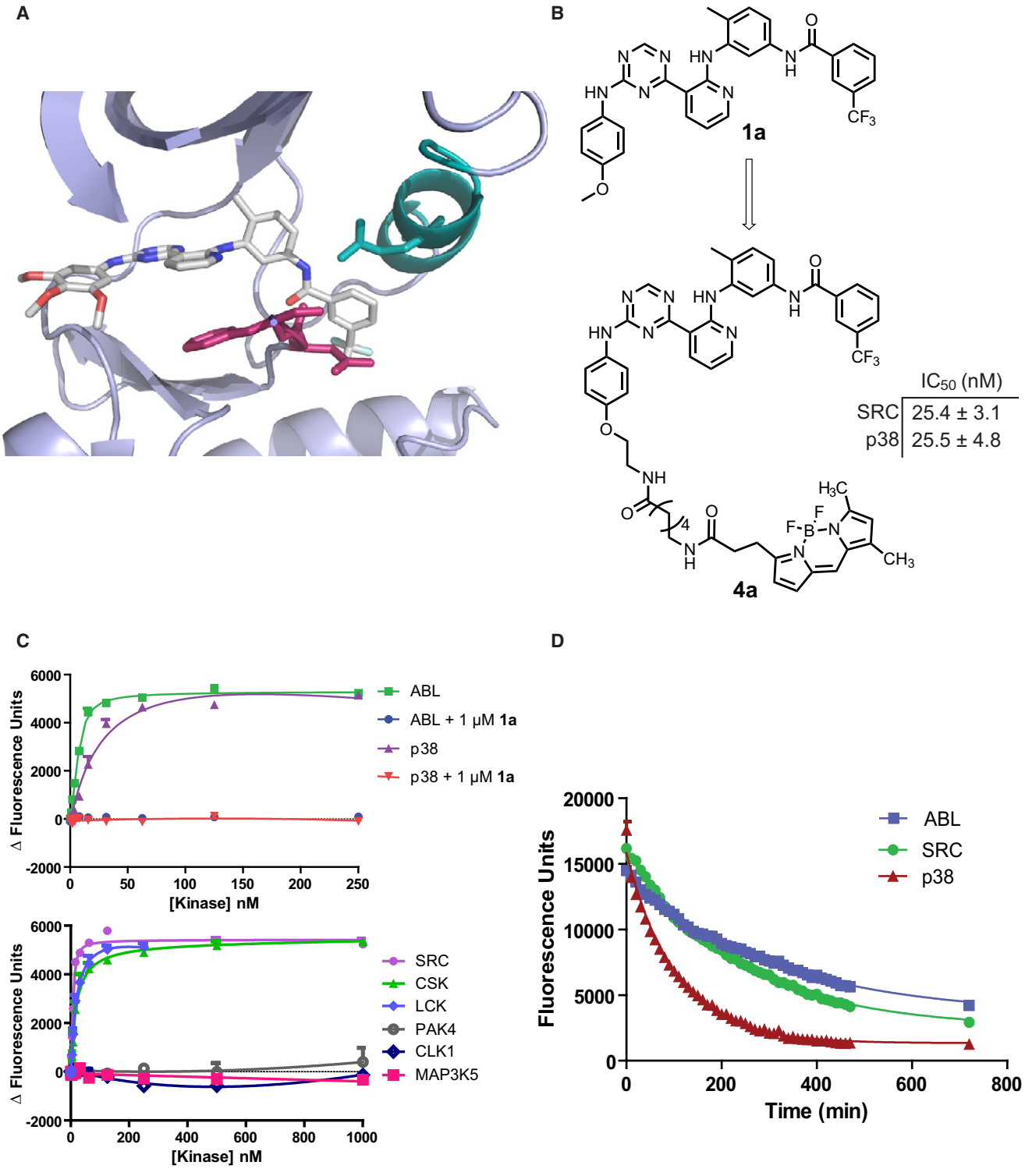

Figure 2. Fluorophore-Labeled Ligands for Studying the Kinetics and Thermodynamics of Type II Inhibitor Binding

(A) Crystal structure of **2a** bound to the catalytic domain of SRC T338I (PDB ID: 3G6H). DFG motif, magenta; helix αC, teal.

(B) Conversion of compound **1a** into a BODIPY-labeled binding probe (**4a**). IC_{50} values of **4a** against SRC and p38 in activity assays.

(C) (Top) Change in fluorescence observed with increasing concentrations of kinases (ABL, green; p38, purple) in the presence of fluorescent probe **4a** (10 nM) and in the presence of both **4a** (10 nM) and competitor **1a** (1000 nM). (Bottom) Change in fluorescence observed with increasing concentrations of the kinases SRC, CSK, LCK, PAK4, CLK1, and MAP3K5 in the presence of **4a** (10 nM).

Table 1. K_d Values of Kinases Determined with 5 nM (ABL, SRC, and HCK) or 10 nM (LCK, p38, CSK, EPHA3, CLK1, PAK4, PAK5, and MAP3K5) 4a

	K_d (nM)
ABL	9.9 ± 1.6
SRC	13 ± 2
HCK	8.7 ± 0.6
LCK	20 ± 2
p38	35 ± 11
CSK	17 ± 3
EPHA3	27 ± 5
CLK1	>1000
PAK4	>1000
PAK5	>1000
MAP3K5	>1000

Values shown are the average of three assays ± SEM.

Table 2. K_d, $t_{1/2}$, and k_{off} Values for Imatinib-Resistant Mutants of ABL and the Corresponding SRC Mutants

Mutants	K_d (nM)	$t_{1/2}$ (min)	k_{off} (s^{-1})
ABL wt	9.9 ± 1.6	220 ± 3	5.2×10^{-5}
ABL E255V	45 ± 4	234 ± 5	4.9×10^{-5}
ABL Y253H	9.4 ± 1.2	195 ± 7	5.9×10^{-5}
SRC wt	13 ± 2	162 ± 4	7.3×10^{-5}
SRC E280V	15 ± 2	133 ± 18	9.0×10^{-5}
SRC F278H	12 ± 3	167 ± 4	6.9×10^{-5}
SRC T338I	11 ± 1	67 ± 9	1.8×10^{-4}
p38	35 ± 11	72 ± 1	1.6×10^{-4}

K_d values for ABL and SRC were determined with 10 nM **4a**. Values shown are the average of three assays ± SEM.

determined (Figure 2C, bottom). Consistent with the in vitro activity assays described above, kinases that have previously been demonstrated to be able to adopt the DFG-out conformation (ABL, SRC, HCK, LCK, p38, EPHA3, and CSK) have a high affinity for probe **4a**, while other kinases (CLK1, PAK4, PAK5, and MAP3K5) do not show a detectable level of binding (Table 1).

Because a large conformational change in the ATP-binding pocket of kinases is required to accommodate inhibitor binding, most type II inhibitors demonstrate slow binding kinetics. To determine if **4a** can be used to obtain type II inhibitor binding kinetics, an assay that allows the measurement of the rate of kinase-**4a** complex dissociation was developed. For this assay, the catalytic domains of SRC, ABL, and p38 were incubated with probe **4a** under conditions in which >95% of the fluorescent probe was bound. The reaction mixture was then diluted 30-fold into a solution containing a large excess of competitor **1a**, to ensure that dissociated **4a** cannot re-bind to the kinase. By measuring the time-dependent loss in fluorescence, the rate of dissociation of the SRC-**4a**, ABL-**4a**, and p38-**4a** complexes were determined (Figure 2D). The data obtained under these conditions fit well to a monoexponential decay curve, with $t_{1/2}$ for the SRC, ABL, and p38 complexes of 162, 220, and 72 min, respectively (Table 2). These data correlate well with kinetic data that has been obtained for this class of compounds and other type II inhibitors (Pargellis et al., 2002; Seeliger et al., 2007, 2009; Sullivan et al., 2005).

We next investigated how mutations in the catalytic domains of protein kinases affect the conformational dynamics of the ATP-binding cleft. Specifically, probe **4a** was used to study how imatinib-resistance mutations in the P-loop affect the interaction of ABL kinase with type II inhibitors (Table 2). The K_d of this probe for two resistance mutants that are frequently observed in patients with chronic myelogenous leukemia that are undergoing imatinib treatment, Y253H and E255V, was determined (Quintas-Cardama et al., 2007). Consistent with inhibitors of this class not making significant interactions with this flexible region of the kinase, the Y253H mutant of ABL was found to have an identical binding affinity for **4a** as the wild-type enzyme. However, the E255V mutant demonstrated a 4- to 5-fold weaker interaction. The analogous mutants of SRC, F278H, and E280V were also characterized. The less flexible nature of SRC's P-loop is reflected in the identical kinetics and thermodynamics observed for both mutants and wild-type. Finally, a gatekeeper mutant of SRC, SRC T338I, was characterized. Similar to the underivatized inhibitor, **4a** has an equal affinity for wild-type and SRC T338I. Despite this similarity in binding thermodynamics, the on and off rates for **4a** are two to three times faster for the gatekeeper mutant.

Generation of Affinity Matrices 14a and 15a

We determined the feasibility of converting compounds **1a** and **3a** into affinity pull-down reagents. These proteomic tools should allow unbiased analyses of the kinases that are able to adopt the DFG-out conformation in diverse cellular lysates. The 4-position of ring A was modified with a flexible polyethylene glycol linker that contains a primary amino group to allow selective immobilization to a solid support (compounds **12a** and **13a**; Figure 3A). Triazolopyridine **12d**, which is an analog of control compound **2d**, was also generated as a negative control for enrichment studies. To determine whether linker attachment affects the potency of this scaffold for kinases that adopt the DFG-out conformation, in vitro activity assays were performed (Figure 3C). Gratifyingly, attachment of a flexible polyethylene glycol linker does not alter the selectivity or potency of these inhibitors. Inhibitor-tethered resins containing **12a** and **13a** were generated by the procedure shown in Figure 3B. In each coupling reaction, the corresponding non-linkable analogs (**1a**, **3a**, or **2d**) were included as controls. Addition of this internal standard allowed the progress of the coupling reaction to be monitored by observing the selective loss of the amine-containing compounds **12a, 13a**, and **12d** by HPLC (see Figures S1 and S2 available online).

(D) Determination of the SRC-**4a**, ABL-**4a**, and p38-**4a** dissociative half-lives ($t_{1/2}$). The catalytic domains of these kinases were incubated under conditions in which >95% of **4a** (500 nM) is bound. The complexes were then diluted 30-fold into a solution containing an excess of competitor **1a** (5 μM) to prevent reformation of the kinase-probe complex. The rate of dissociation is measured by the decrease in fluorescence over time. Fluorescence was read every 10 min for 8 hr, and then at 12 hr. Data was fit to a monoexponential decay curve. Assays were run in triplicate.

A

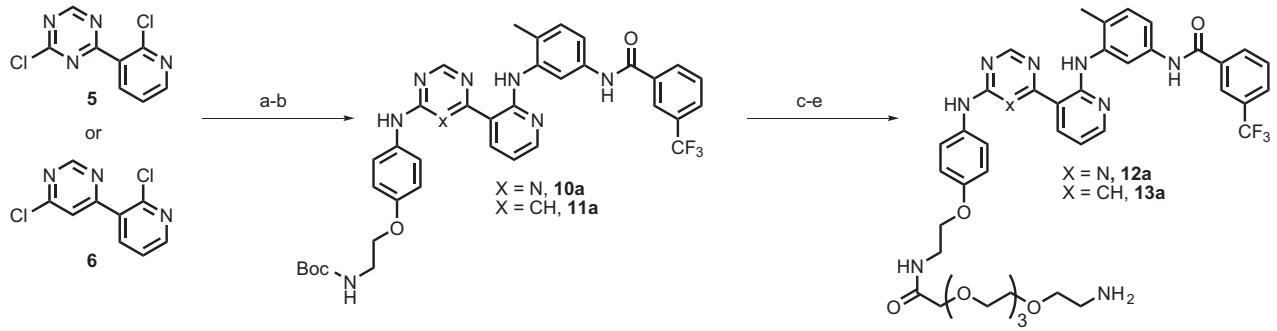

Reagents and Conditions: (a) if X = N; (i) **7**, *i*-PrOH, rt; (ii) TEA, rt; if X= CH; **7**, EtOH, 80°C; (b) **8**, Et_3N-TFA, DMSO, 95°C; (c) 30% TFA, CH_2Cl_2, rt; (d) **9**, HOBt, EDC, DIEA, CH_2Cl_2, rt; (e) 30% TFA, CH_2Cl_2, rt

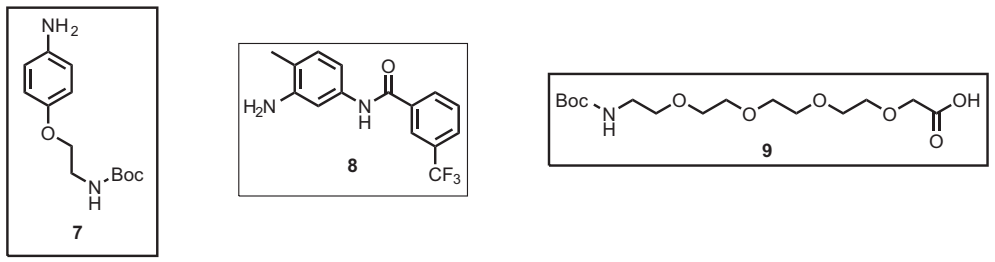

B

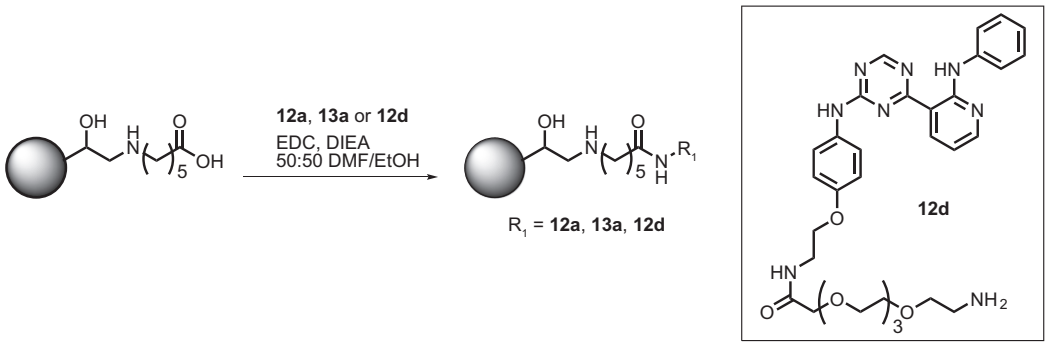

C

IC_{50} (nM)

	ABL	SRC	HCK	LCK	p38	CSK	PKA	CLK1	PAK4	PAK5	MAP3K5	IRAK4	ERK2
12a	6.6 ± 0.5	3.3 ± 0.6	9.6 ± 0.4	< 10	< 13	16.3 ± 1.6	> 10000	> 10000	> 10000	> 10000	> 10000	> 10000	> 10000
13a	6.6 ± 1.0	5.7 ± 3.1	6.3 ± 1.4	< 10	< 13	140 ± 9	> 10000	> 10000	> 10000	> 10000	> 10000	> 10000	> 10000

Figure 3. Synthesis and Characterization of Immobilized type II Inhibitors
(A) Synthetic scheme for generating type II inhibitors that can be immobilized.
(B) Procedure for generating affinity matrices **14a** (R_1 = **12a**), **14d** (R_1 = **12d**), and **15a** (R_1 = **13a**).
(C) IC_{50}s of inhibitors **12a** and **13a** against a panel of kinases.

Affinity Matrices 14a and 15a Enrich Kinases that Adopt the DFG-Out Conformation

A model system was developed to determine the ability of affinity matrices **14a** and **15a** to enrich kinases that are able to adopt the DFG-out conformation. Optimal conditions for affinity capture, resin washing, and protein elution were determined by adding purified protein kinases to cellular lysates from *E. coli* (Figures 4A and 4B). Because *E. coli* lack eukaryotic and eukaryotic-like protein kinases, only exogenously added kinases should be retained by the affinity matrix (Kannan et al., 2007). We first tested the ability of affinity matrix **15a** to enrich p38 kinase from lysates. A majority of His6-p38 was retained by affinity matrix **15a** after 2 hr of incubation as demonstrated by the lack of detectable levels of His6-tagged kinase in the soluble fraction (Figure 4A).

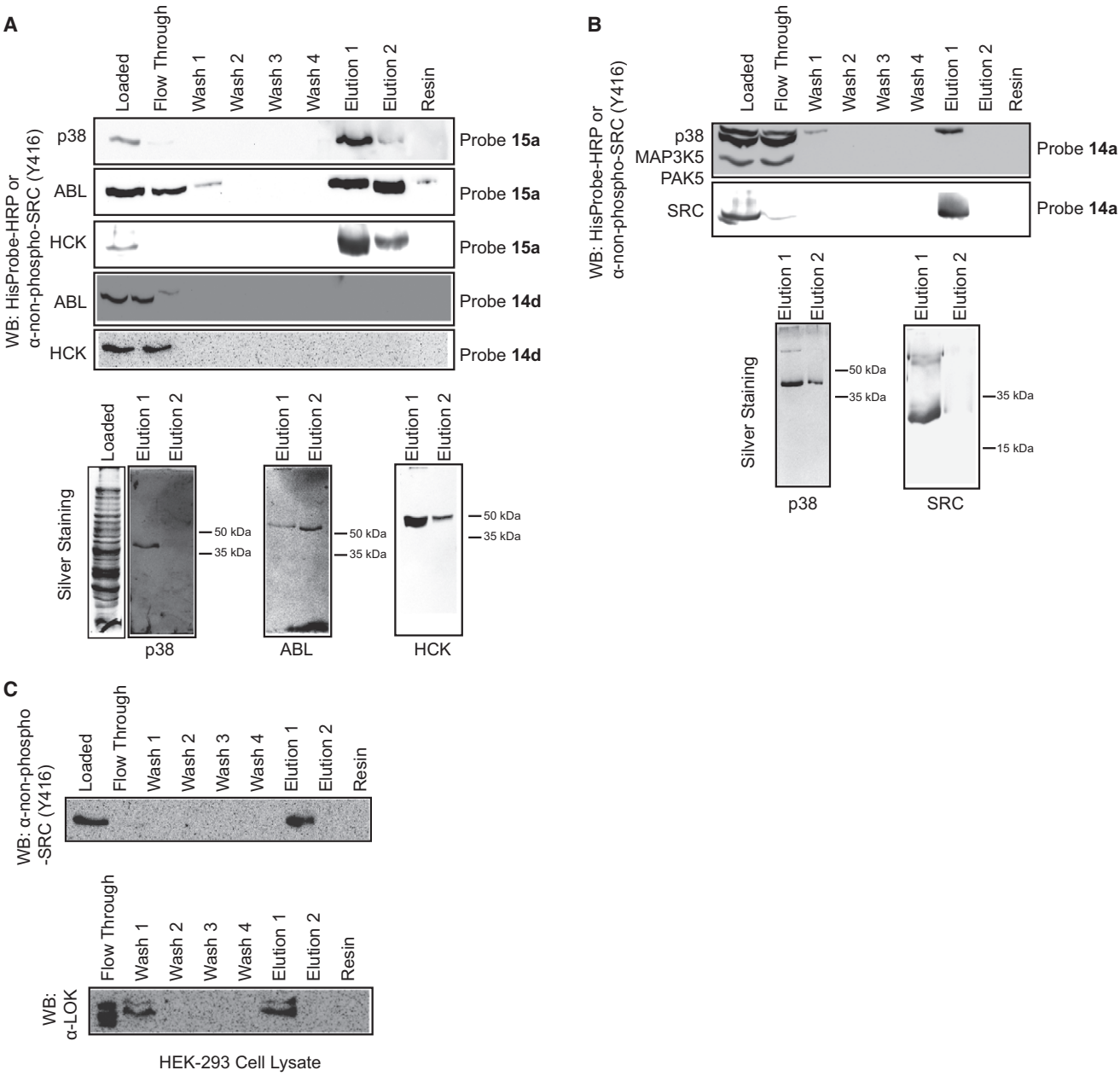

Figure 4. Characterization of Immobilized Type II Inhibitors 14a and 15a

(A) Enrichment of protein kinases from *E.* coli lysates with affinity resins **14a** or **15a** or control matrix **14d**. Purified His6-p38 (4.6 μg), His6-ABL (5 μg), or HCK (18 μg) were added to *E. coli* lysate (550–700 μg) and subjected to standard enrichment conditions with affinity matrix **15a** or control matrix **14d**. (Top) All fractions were subjected to SDS-PAGE. ABL and p38 were detected with HisProbe-HRP (Pierce); SRC and HCK were detected with an antibody that specifically recognizes SRC-family kinases that are dephosphorylated at Tyr416 in the activation loop [α-non-phospho-SRC(Y416)] (Cell Signaling). (Bottom) Elutions 1 and 2 from the enrichment experiments described above were subjected to SDS-PAGE and silver stained.

(B) Enrichment of kinases that are sensitive to type II inhibitors in the presence of kinases that have not been characterized in the DFG-out conformation. His6-p38 (4 μg), His6-MAP3K5 (10 μg), and His6-PAK5 (10 μg) were added to *E. coli* lysate (500 μg) and subjected to standard enrichment conditions with affinity matrix **14a**. The catalytic domain of SRC (4 μg), His6-MAP3K5 (4.5 μg), and His6-STK16 (4.5 μg) were added to *E. coli* lysate (600 μg) and subjected to standard enrichment conditions with affinity matrix **14a**. (Top) All fractions were subjected to SDS-PAGE and probed with HisProbe-HRP or α-non-phospho-SRC(Y416). (Bottom) Elutions 1 and 2 from the enrichment experiments described above were subjected to SDS-PAGE and silver stained. Note: Procedures for protein kinase expression and purification are in the Supplemental Experimental Procedures.

(C) Enrichment of endogenous kinases from HEK293 cell lysate. 600 μg of HEK293 lysate was subjected to standard enrichment conditions with affinity matrix **14a**. All fractions were subjected to SDS-PAGE and probed with α-non-phospho-SRC(Y416) or α-LOK.

Furthermore, no immobilized p38 was found to dissociate from the resin after multiple washes. Repeated efforts to elute p38 from the affinity matrix with high concentrations of soluble, ATP-competitive inhibitors were unsuccessful. This is most likely due to the high affinity of the immobilized ligand for kinases that adopt the DFG-out conformation and the slow rate of dissociation of these inhibitor-kinase complexes. However, a mild denaturant (0.5% SDS) allowed quantitative elution of this kinase. Furthermore, these conditions appear to be selective for disruption of the kinase-inhibitor complex as demonstrated by the lack of other proteins in the eluted fractions detected via silver staining. The same conditions were found to be effective for enriching ABL and the SRC family kinase HCK (Figure 4A). As expected, none of these kinases were retained by control matrix **14d**. To ensure that the affinity matrix selectively enriches kinases that adopt the DFG-out conformation, p38 was subjected to the standard affinity enrichment protocol in an *E. coli* protein lysate containing the kinases PAK5 and MAP3K5 (Figure 4A). As expected, only p38 was bound and retained by affinity matrix **14a**. Furthermore, p38 was the only protein that could be detected in the eluted fractions. Similar results were observed for SRC.

The ability of immobilized inhibitor **14a** to enrich endogenous protein kinases from mammalian lysates was tested. Western blot analysis demonstrated that >90% of total SRC was retained by the beads when 650 μg of HEK293 protein lysate was incubated with affinity resin **14a** (Figure 4C). SRC remained bound to the affinity matrix during repeated washes and was eluted with 0.5% SDS. Comparison of the proteins eluted from control matrix **14d** and affinity matrix **14a** by SDS-PAGE followed by silver staining demonstrated that several unique proteins were enriched from HEK293 and HeLa cell lysates by immobilized inhibitor **14a** (Figure S3). However, a number of prominent bands were present in the eluted fractions for both support-bound ligands. These appear to be proteins that bind nonspecifically to the matrix, as preincubation with control matrix **14d** prior to enrichment with **14a** did not deplete a majority of these bands. Mass spectrometric analysis of the proteins that were enriched from HEK293 and HeLa cells is ongoing and will be reported elsewhere. In parallel, a candidate approach for identifying kinases that can adopt the DFG-out conformation was pursued. Previous inhibitor screens have shown that the serine/threonine kinase LOK is sensitive to several type II inhibitors (Angell et al., 2008; Fabian et al., 2005; Karaman et al., 2008). However, biochemical studies have not been performed to establish whether LOK can adopt the DFG-out conformation. To determine whether endogenous LOK binds to the triazolopyridine scaffold, HEK293 cell lysate was incubated with affinity matrix **14a**. Immunoblot analysis of the bound and unbound fractions with an α-LOK antibody demonstrated that a percentage of this kinase was retained by the beads and selectively eluted.

The Catalytic Domain of LOK Behaves Similarly to Other DFG-Out-Adopting Protein Kinases

To further characterize LOK, the His6-tagged catalytic domain of this kinase was expressed and purified using a previously described protocol (Fedorov et al., 2007). An in vitro activity assay was developed for LOK and compounds **1a-c**, **2a**, and **3a** were tested for their ability to inhibit this kinase. LOK was found to be equally sensitive to inhibition by type II inhibitors as other kinases that adopt the DFG-out conformation (Table S1). Furthermore, resins **14a** and **15a** were able to enrich the catalytic domain of LOK from *E. coli* lysate over other protein kinases (Figure 5A). In addition, LOK was not retained by control matrix **14d**. To further confirm the affinity of LOK for the type II inhibitor class, binding studies with probe **4a** were performed. Similar to other kinases that adopt the DFG-out conformation, LOK has a high affinity for this fluorescently-labeled probe (K_d = 12 nM; Figure 5B). Finally, the $t_{1/2}$ for the LOK-**4a** complex was determined (Figure 5C). Consistent with LOK demonstrating slow binding kinetics for type II inhibitors, the $t_{1/2}$ for this complex was found to be 51 min. Although the off rate for probe **4a** is 3- to 4-fold faster than for SRC and ABL, the kinetics observed are consistent with a conformational change being necessary for ligand binding.

DISCUSSION

After it was discovered that the inhibitors imatinib and BIRB796 bind to the inactive forms of their kinase targets, there has been widespread interest in the identification of small molecules that selectively recognize alternate active site conformations (Liu and Gray, 2006; Nagar et al., 2002; Okram et al., 2006; Schindler et al., 2000). High selectivity can be achieved with inhibitors that bind to inactive kinase conformations and the characteristically long target residence times of these protein-small molecule complexes may be beneficial from a therapeutic standpoint. The DFG-out conformation is a specific inactive form that has been successfully targeted by a number of type II inhibitors. While it was once thought that only a few kinases are able to adopt this conformation, recent studies have demonstrated that it is accessible to many members of the human kinome (Choi et al., 2009; Dar et al., 2008; DiMauro et al., 2006; Han et al., 2009; Hodous et al., 2007; Mol et al., 2004; Schroeder et al., 2009; Seeliger et al., 2009; Wan et al., 2004). However, the sequence and structural determinants that allow a kinase to adopt the DFG-out conformation are still not known and it is not possible to predict which kinases will be sensitive to type II inhibitors. To address this issue, our goal was to identify a general ligand for kinases that adopt the DFG-out conformation. We have found that compounds based on the triazolopyridine scaffold, which we have previously demonstrated through kinetic and structural studies to bind the DFG-flipped forms of the kinases ABL and SRC, potently inhibit a broad spectrum of kinases that are sensitive to type II inhibitors. Furthermore, these compounds do not inhibit other well-characterized kinases that have not previously been observed in this specific inactive form.

A small panel of analogs based on the triazolopyridine scaffold was generated to determine how substituents that occupy the pocket created by the DFG motif flipping to a more solvent exposed position affect kinase selectivity (Figure 1). As expected, a control compound that lacks a hydrophobic moiety that occupies the DFG-out pocket and an amide group that makes a set of characteristic hydrogen bonds with the backbone amide of the DFG motif and a conserved glutamic acid in the helix αC does not inhibit any of the DFG-out-adopting kinases. Furthermore, an analog that contains a 3-trifluormethylbenzamide (**1a**), which is a general pharmacophore that occupies the DFG-out pocket in many type II inhibitors, appears to be

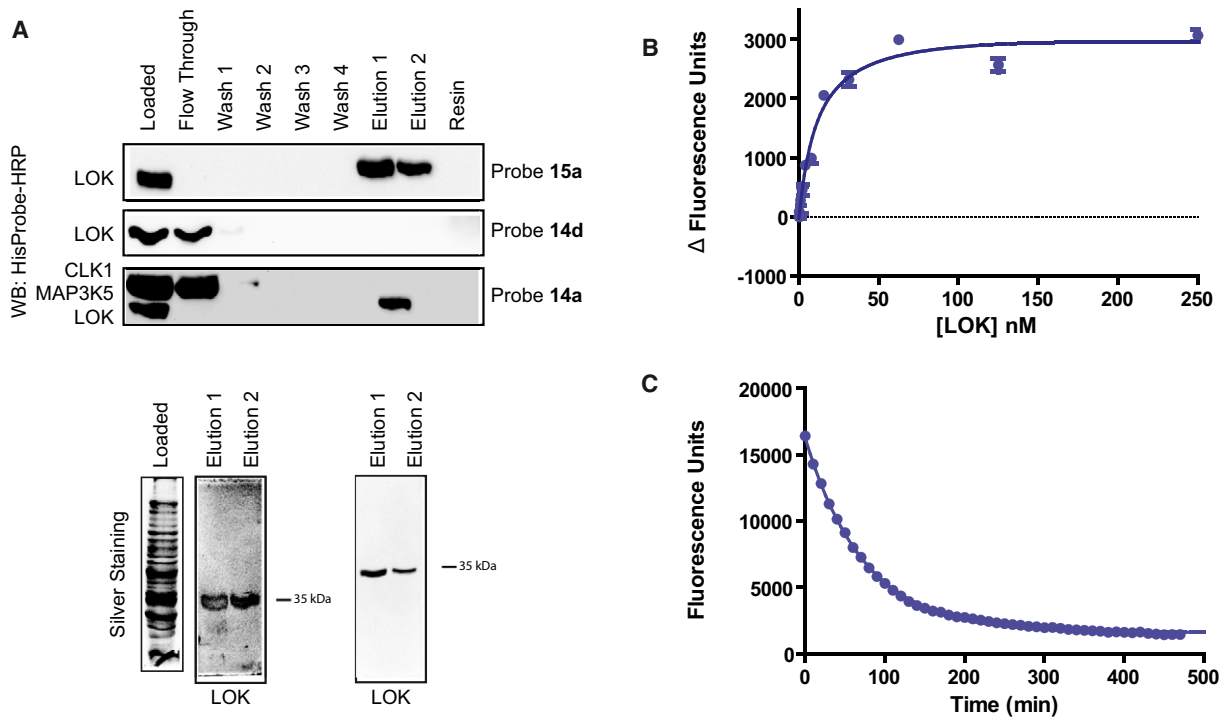

Figure 5. The Catalytic Domain of LOK Behaves Like a Kinase that Can Adopt the DFG-Out Conformation

(A) Enrichment of the catalytic domain of LOK from *E. coli* lysates with affinity resins **14a** or **15a** or control matrix **14d**. (Top) Purified His6-LOK (4.5 μg) was added to *E. coli* lysate (600 μg) and subjected to standard enrichment conditions with affinity matrix **15a**. LOK was detected with HisProbe-HRP (Pierce). (Middle) Purified His6-LOK (4.5 μg) was added to *E. coli* lysate (600 μg) and subjected to standard enrichment conditions with control matrix **14d**. LOK was detected with HisProbe-HRP. (Bottom) Purified His6-LOK (4 μg), His6-CLK1 (10 μg), and His6-MAP3K5 (10 μg) were added to *E. coli* lysate (500 μg) and subjected to standard enrichment conditions with affinity matrix **14a**. All fractions were subjected to SDS-PAGE and kinases were detected with HisProbe-HRP (Pierce). (Bottom gels) Elutions 1 and 2 from the enrichment experiments performed in the top and bottom panels above. Samples were subjected to SDS-PAGE and silver stained.

(B) Change in fluorescence observed with an increasing concentration of LOK in the presence of 5 nM of fluorescent probe **4a**. $K_d = 12 \pm 1$ nM. Value shown is the average of three assays ± SEM.

(C) Determination of the LOK-**4a** complex dissociative half-life ($t_{1/2}$). For LOK-**4a**, $t_{1/2} = 51$ min and $k_{off} = 2.3 \times 10^{-5}$ s^{-1}. Assays were run in triplicate.

a nonselective ligand for kinases that have previously been characterized to adopt the DFG-out conformation. Unexpectedly, replacing this pharmacophore with functional groups from more selective type II inhibitors does not greatly enhance the selectivity profile for compounds based on the triazolopyridine scaffold. For example, compound **1b**, which contains a 2-morphilinopyridyl group, is a nearly equipotent inhibitor of p38, ABL, SRC, HCK, and CSK; however, inhibitors that display this moiety from a 4-anilinoquinazoline scaffold are >500-fold selective for p38 over these kinases (Perera and Maly, 2008). Similarly, **1c**, which contains the functional groups present in the highly selective BCR-ABL inhibitor nilotinib, is a fairly nonselective inhibitor of DFG-out-adopting kinases. These data highlight that the ability of some type II inhibitors to discriminate between closely related kinases is most likely due to several unique protein-ligand interactions rather than a single selectivity filter. Indeed, we have demonstrated that a unique interaction between the P-loop of ABL and imatinib makes a major contribution to the ability of this compound to inhibit this kinase over closely related SRC (Seeliger et al., 2009). Several recent reports that describe type II inhibitors with limited selectivity profiles highlight that ligands of this class have the potential to inhibit a much broader spectrum of kinases than was previously appreciated (Angell et al., 2008; Choi et al., 2009; Okram et al., 2006).

To gain a better understanding of how inhibitors based on the triazolopyridine scaffold interact with protein kinases, we converted compound **1a** into a fluorescently-labeled ligand that can be used in binding assays (Figure 2). The use of a binding assay allows the affinity of this probe to be determined for kinases in any activation state and facilitates the direct measurement of ligand binding kinetics. As many type II inhibitors have long residence times and slow on rates, determination of slow binding kinetics with a general probe for the DFG-out conformation can be used to verify the ability of a kinase to adopt this inactive form. In the presence of DFG-out-adopting kinases, fluorescent probe **4a** demonstrated a concentration-dependent increase in fluorescence. An assay was developed to measure the residence time of this probe when bound to p38, SRC, and ABL. The slow binding kinetics demonstrated by this probe are similar to those observed for other type II inhibitors of these kinases (Pargellis et al., 2002; Seeliger et al., 2007, 2009; Sullivan et al., 2005). This assay was also used to study how drug-resistance mutations affect the interactions of kinases with type II inhibitors. A mutation to the flexible P-loop region of ABL,

E255V, was found to reduce the affinity of this kinase for the probe. Interestingly, the observed loss in affinity is due to a slower on rate rather than a slower rate of dissociation. None of the analogous P-loop mutations in SRC were found to affect the interaction of this kinase with type II inhibitors, which is consistent with this region not interacting with inhibitors. Finally, mutation of the gatekeeper residue of SRC to a bulkier residue was found to affect both the on and off rates of ligand binding. This result is consistent with recent findings that mutation of the gatekeeper residue in ABL causes increased conformational disturbances in a specific catalytic domain region of this kinase (Iacob et al., 2009).

While structural studies and kinetic assays can be used to determine if a kinase can adopt the DFG-out conformation, these methods can only be performed on purified proteins. Because it is difficult to know whether the conformational preferences of a recombinantly expressed purified kinase are representative of those in a cell, probes that allow interrogation of endogenous kinases are highly desirable. For this reason, we developed a support-bound affinity matrix based on inhibitor **1a** that allows an unbiased sampling of mammalian lysates. We first verified that our affinity matrix was capable of enriching purified kinases that are known to be sensitive to type II inhibitors from complex mixtures (Figure 4). Indeed, affinity matrices **14a** and **15a** selectively enriched SRC, HCK, and p38 from an *E. coli* lysate but not kinases that are insensitive to type II inhibitors. Importantly, control matrix **14d**, which does not contain a pharmacophore that occupies the DFG-out pocket, does not enrich any of the kinases tested. We next tested this reagent in mammalian cell lysates. First, it was verified that affinity matrix **14a** was able to enrich endogenous SRC from HEK293 cells. Analysis of the proteins that were selectively enriched with affinity resin **14a** over control matrix **14d** from HeLa and HEK293 lysates demonstrated that there are several unique proteins. Mass spectrometric identification of these proteins is currently being performed.

A candidate approach using western blot analysis was adopted to discover novel DFG-out-adopting kinases. We found that the STE20 kinase LOK could be selectively enriched from HEK293 lysates with affinity matrix **14a**. Furthermore, the purified catalytic domain could be enriched from *E. coli* lysates and was sensitive (IC_{50} < 20 nM) to type II inhibitors **1a**-**1c**, **2a**, and **3a** in activity assays (Table S1). Finally, LOK demonstrated similarly slow binding kinetics with type II inhibitors such as ABL, SRC, and p38. Besides p38 and RAF, no other serine/threonine kinases have been characterized in the DFG-out conformation. Furthermore, no members of the STE20 kinase family have been found to be sensitive to type II inhibitors. Indeed, MAP3K5, PAK4, and PAK5, which are STE20 kinases and much more closely related to LOK than SRC or ABL, were not sensitive to any of the affinity reagents that we have developed. LOK is also of interest because it contains a residue with a bulky side chain (isoleucine) at the gatekeeper position. To date, a vast majority of the kinases that have been characterized to adopt the DFG-out conformation (except Tie-2, PYK2, and c-MET) contain either a threonine or valine at this position. However, the presence of a larger gatekeeper residue does not preclude a kinase from adopting this form. While conversion of the threonione gatekeeper of ABL to an isoleucine results in this kinase being resistant to the type II inhibitors imatinib and nilotinib, several type II inhibitors that are extremely potent against this mutant have been described (Huang et al., 2009; O'Hare et al., 2009; Seeliger et al., 2009). Expanding the number and diversity of kinases that are known to stably adopt the DFG-out conformation will allow the identification of the sequence determinants that allow this transition.

SIGNIFICANCE

A number of type II inhibitors have been developed that target an inactive form of the ATP-binding site of kinases called the DFG-out conformation. Once thought to be energetically accessible to only a few kinases, the DFG-out conformation has been characterized with an increasing number of enzymes from this family. However, it is still not possible to predict which members of the kinome are able to stably adopt this inactive conformation. In addition, the structural and sequence determinants of this transition remain poorly understood. Here, we have identified a scaffold that appears to be a general pharmacophore for the DFG-out conformation. Derivatives of this scaffold are potent inhibitors of kinases that have previously been characterized to be sensitive to type II inhibitors. Furthermore, fluorophore-conjugated versions of these molecules allow the determination of the thermodynamics and kinetics of ligand binding to any activation state of the kinase catalytic domain. In addition, immobilized analogs of the general scaffold were found to be effective reagents for enriching DFG-out-adopting kinases from complex protein mixtures. Affinity reagents 14a and 15a were used to demonstrate that the STE20 kinase LOK behaves like other DFG-out-adopting kinases. LOK is distantly related to other members of the kinase family that have been characterized in the DFG-out conformation. Use of these reagents to discover the full complement of kinases that are able to stably adopt the DFG-out conformation will allow a greater understanding of the thermodynamics and kinetics of the catalytic domains of this enzyme family.

EXPERIMENTAL PROCEDURES

Synthetic Methods

Detailed synthetic procedures are in the Supplemental Experimental Procedures.

Affinity Measurements with Probe 4a

Purified kinase (initial concentration = 250 nM, 2-fold serial dilution down to 0.2 nM) was incubated with 5 or 10 nM **4a** in 120 μl of buffer containing 20 mM Tris (pH 7.5), 2% DMSO, 100 mM KCl, 10% glycerol, 1 mM DTT, 0.05% Pluronic F-68, and 1 mM $MgCl_2$. Fluorescence was read after 30 min of incubation at room temperature (excitation = 485 nm; emission = 535 nm). The K_d was determined by fitting the data to non-linear regression analysis (one site total binding) with Prism GraphPad software.

Determination of $t_{1/2}$ with Probe 4a

Purified kinase (700 nM) was incubated with **4a** (500 nM) in 120 μl of buffer containing 20 mM Tris (pH 7.5), 2% DMSO, 100 mM KCl, 10% glycerol, 1 mM DTT, 0.05% Pluronic F-68, and 1 mM $MgCl_2$. After 4 hr, the mixture was diluted 30-fold ([**4a**] = 17 nM) into the same buffer containing 5 μM of **1a**. Fluorescence was read every 10 min for 8 hr, and then at 12 hr (excitation = 485 nm; emission = 535 nm). Off rates (k_{off}) and dissociative half-lives ($t_{1/2}$) were determined

by fitting the data to a one phase exponential decay equation with Prism GraphPad software.

Generation of Affinity Matrix 14a

A modification of a previously published procedure was used (Wissing et al., 2007). 1.5 ml of ECH Sepharose resin was washed with 10 bed volumes of H_2O (pH 4.5; 0.5 M NaCl) and 1:1 DMF/EtOH. 3 ml of 0.75 mM **12a** and 0.46 mM **1a** in 1:1 DMF/EtOH was added to the resin followed by 30 μl of DIEA and 450 μl of 1 M EDCI in 1:1 DMF/EtOH. The reaction mixture was rotated for 48 hr and monitored by analytical HPLC (Figures S2 and S3). After 48 hr, the reaction mixture was drained and washed with 2 bed volumes of 1:1 DMF/EtOH. The resin was then incubated with 56 μl ethanolamine, 933 μl of 20 mM acetic acid, and 450 μl of EDCI in 1:1 DMF/EtOH for 12 hr, followed by washing with 6 bed volumes of 1:1 DMF/EtOH (3×), 6 bed volumes of 0.5 M NaCl (2×), and 10 bed volumes of 20% EtOH. The resin was stored at 4°C in 20% EtOH until further use. Affinity matrices **14d** and **15a** were generated by the same method.

General Method for Affinity Enrichment from *E. coli* Lysate

50 μl of affinity matrix **14a**, **14d**, or **15a** was washed with 8 bed volumes of a buffer containing 50 mM HEPES (pH 7.5), 0.5% Triton X-100, 1 mM EDTA, 1 mM EGTA, and 100 mM NaCl. Purified kinase (4–18 μg) and *E. coli* lysate protein (500–800 μg) in 250 μl of binding buffer [50 mM HEPES (pH 7.5), 0.5% Triton X-100, 1 mM EDTA, 1 mM EGTA, 20 mM $MgCl_2$, 1 M NaCl, and 100 μg/ml PMSF] was added to the resin and incubated for 2 hr at 4°C. The resin was then drained, incubated with 8 bed volumes of binding buffer for 30 min at 4°C, and drained again (4 washes). After the final wash, 1.5 bed volumes of 0.5% SDS in binding buffer was added to the resin and incubated for 10 min at room temperature. The eluted protein was collected and this process was repeated. All collected fractions were subjected to SDS-PAGE, transferred to nitrocellulose, and subjected to western blot analysis. Eluted fractions were also subjected to SDS-PAGE and stained with Silver Stain Xpress (Invitrogen).

General Method for Affinity Enrichment from Mammalian Cell Lysate

50–150 μl of affinity matrix **14a**, **14d**, or **15a** was washed with 8 bed volumes of a buffer containing 50 mM HEPES (pH 7.5), 0.5% Triton X-100, 1 mM EDTA, 1 mM EGTA, and 100 mM NaCl. HEK293 or HeLa lysate proteins (0.6–8 mg) in 0.25–1.0 ml of buffer containing 50 mM HEPES (pH 7.5), 0.5% Triton X-100, 1 mM EDTA, 1 mM EGTA, 2.5 mM sodium orthovanadate, 1 mM PMSF, Roche protease inhibitor cocktail, and 20 mM $MgCl_2$ was added to the resin and incubated for 2 hr at 4°C. The resin was then drained, incubated with 8 bed volumes of binding buffer for 30 min at 4°C, and drained again (4 washes). After the final wash, 3–4 bed volumes of 0.5% SDS in binding buffer was added to the resin and incubated for 10 min at room temperature. The eluted protein was collected and this process was repeated. All collected fractions were lyophilized, subjected to SDS-PAGE, transferred to nitrocellulose, and subjected to western blot analysis with an α-non-phospho-SRC(Y416) or α-LOK antibody. Eluted fractions were subjected to SDS-PAGE and stained with Silver Stain Xpress.

SUPPLEMENTAL DATA

Supplemental Data include Supplemental Experimental Procedures, three figures, and one table and can be found with this article online at doi:10.1016/j.chembiol.2010.01.008.

ACKNOWLEDGMENTS

We thank J. Kuriyan (University of California, Berkeley) and M. Seeliger (State University of New York, Stony Brook) for providing expression plasmids for ABL (cat), SRC (cat), HCK (cat), HCK (3D), LCK (3D), SRC (3D), and ABL (3D). We thank S. Knapp (Structural Genomics Consortium) for providing expression plasmids for CLK1, STK16, EPHA3, PAK4, PAK5, MAP3K5, and LOK. This work was supported by the National Institute of General Medical Science (R01GM086858 to D.J.M.).

Received: December 1, 2009
Revised: January 18, 2010
Accepted: January 20, 2010
Published: February 25, 2010

REFERENCES

Angell, R.M., Angell, T.D., Bamborough, P., Bamford, M.J., Chung, C.W., Cockerill, S.G., Flack, S.S., Jones, K.L., Laine, D.I., Longstaff, T., et al. (2008). Biphenyl amide p38 kinase inhibitors 4: DFG-in and DFG-out binding modes. Bioorg. Med. Chem. Lett. *18*, 4433–4437.

Choi, Y., Syeda, F., Walker, J.R., Finerty, P.J., Jr., Cuerrier, D., Wojciechowski, A., Liu, Q., Dhe-Paganon, S., and Gray, N.S. (2009). Discovery and structural analysis of Eph receptor tyrosine kinase inhibitors. Bioorg. Med. Chem. Lett. *19*, 4467–4470.

Cohen, P. (2000). The regulation of protein function by multisite phosphorylation—a 25 year update. Trends Biochem. Sci. *25*, 596–601.

Cohen, P. (2002). Protein kinases—the major drug targets of the twenty-first century? Nat. Rev. Drug Discov. *1*, 309–315.

Cumming, J.G., McKenzie, C.L., Bowden, S.G., Campbell, D., Masters, D.J., Breed, J., and Jewsbury, P.J. (2004). Novel, potent and selective anilinoquinazoline and anilinopyrimidine inhibitors of p38 MAP kinase. Bioorg. Med. Chem. Lett. *14*, 5389–5394.

Dar, A.C., Lopez, M.S., and Shokat, K.M. (2008). Small molecule recognition of c-Src via the Imatinib-binding conformation. Chem. Biol. *15*, 1015–1022.

DiMauro, E.F., Newcomb, J., Nunes, J.J., Bemis, J.E., Boucher, C., Buchanan, J.L., Buckner, W.H., Cee, V.J., Chai, L., Deak, H.L., et al. (2006). Discovery of aminoquinazolines as potent, orally bioavailable inhibitors of Lck: synthesis, SAR, and in vivo anti-inflammatory activity. J. Med. Chem. *49*, 5671–5686.

Engh, R.A., and Bossemeyer, D. (2001). The protein kinase activity modulation sites: mechanisms for cellular regulation - targets for therapeutic intervention. Adv. Enzyme Regul. *41*, 121–149.

Fabian, M.A., Biggs, W.H., III, Treiber, D.K., Atteridge, C.E., Azimioara, M.D., Benedetti, M.G., Carter, T.A., Ciceri, P., Edeen, P.T., Floyd, M., et al. (2005). A small molecule-kinase interaction map for clinical kinase inhibitors. Nat. Biotechnol. *23*, 329–336.

Fedorov, O., Marsden, B., Pogacic, V., Rellos, P., Muller, S., Bullock, A.N., Schwaller, J., Sundstrom, M., and Knapp, S. (2007). A systematic interaction map of validated kinase inhibitors with Ser/Thr kinases. Proc. Natl. Acad. Sci. USA *104*, 20523–20528.

Han, S., Mistry, A., Chang, J.S., Cunningham, D., Griffor, M., Bonnette, P.C., Wang, H., Chrunyk, B.A., Aspnes, G.E., Walker, D.P., et al. (2009). Structural characterization of proline-rich tyrosine kinase 2 (PYK2) reveals a unique (DFG-out) conformation and enables inhibitor design. J. Biol. Chem. *284*, 13193–13201.

Hanks, S.K., and Hunter, T. (1995). Protein kinases 6. The eukaryotic protein kinase superfamily: kinase (catalytic) domain structure and classification. FASEB J. *9*, 576–596.

Hodous, B.L., Geuns-Meyer, S.D., Hughes, P.E., Albrecht, B.K., Bellon, S., Bready, J., Caenepeel, S., Cee, V.J., Chaffee, S.C., Coxon, A., et al. (2007). Evolution of a highly selective and potent 2-(pyridin-2-yl)-1,3,5-triazine Tie-2 kinase inhibitor. J. Med. Chem. *50*, 611–626.

Huang, W.S., Zhu, X., Wang, Y., Azam, M., Wen, D., Sundaramoorthi, R., Thomas, R.M., Liu, S., Banda, G., Lentini, S.P., et al. (2009). 9-(Arenethenyl)-purines as dual Src/Abl kinase inhibitors targeting the inactive conformation: design, synthesis, and biological evaluation. J. Med. Chem. *52*, 4743–4756.

Huse, M., and Kuriyan, J. (2002). The conformational plasticity of protein kinases. Cell *109*, 275–282.

Iacob, R.E., Pene-Dumitrescu, T., Zhang, J., Gray, N.S., Smithgall, T.E., and Engen, J.R. (2009). Conformational disturbance in Abl kinase upon mutation and deregulation. Proc. Natl. Acad. Sci. USA *106*, 1386–1391.

Jacobs, M.D., Caron, P.R., and Hare, B.J. (2008). Classifying protein kinase structures guides use of ligand-selectivity profiles to predict inactive conformations: structure of lck/imatinib complex. Proteins *70*, 1451–1460.

Jeffrey, P.D., Russo, A.A., Polyak, K., Gibbs, E., Hurwitz, J., Massague, J., and Pavletich, N.P. (1995). Mechanism of CDK activation revealed by the structure of a cyclinA-CDK2 complex. Nature *376*, 313–320.

Kannan, N., Taylor, S.S., Zhai, Y., Venter, J.C., and Manning, G. (2007). Structural and functional diversity of the microbial kinome. PLoS Biol. *5*, e17.

Karaman, M.W., Herrgard, S., Treiber, D.K., Gallant, P., Atteridge, C.E., Campbell, B.T., Chan, K.W., Ciceri, P., Davis, M.I., Edeen, P.T., et al. (2008). A quantitative analysis of kinase inhibitor selectivity. Nat. Biotechnol. *26*, 127–132.

Kornev, A.P., Haste, N.M., Taylor, S.S., and Eyck, L.F. (2006). Surface comparison of active and inactive protein kinases identifies a conserved activation mechanism. Proc. Natl. Acad. Sci. USA *103*, 17783–17788.

Liu, Y., and Gray, N.S. (2006). Rational design of inhibitors that bind to inactive kinase conformations. Nat. Chem. Biol. *2*, 358–364.

Manning, G., Whyte, D.B., Martinez, R., Hunter, T., and Sudarsanam, S. (2002). The protein kinase complement of the human genome. Science *298*, 1912–1934.

Mol, C.D., Dougan, D.R., Schneider, T.R., Skene, R.J., Kraus, M.L., Scheibe, D.N., Snell, G.P., Zou, H., Sang, B.C., and Wilson, K.P. (2004). Structural basis for the autoinhibition and STI-571 inhibition of c-Kit tyrosine kinase. J. Biol. Chem. *279*, 31655–31663.

Nagar, B., Bornmann, W.G., Pellicena, P., Schindler, T., Veach, D.R., Miller, W.T., Clarkson, B., and Kuriyan, J. (2002). Crystal structures of the kinase domain of c-Abl in complex with the small molecule inhibitors PD173955 and imatinib (STI-571). Cancer Res. *62*, 4236–4243.

O'Hare, T., Shakespeare, W.C., Zhu, X., Eide, C.A., Rivera, V.M., Wang, F., Adrian, L.T., Zhou, T., Huang, W.S., Xu, Q., et al. (2009). AP24534, a pan-BCR-ABL inhibitor for chronic myeloid leukemia, potently inhibits the T315I mutant and overcomes mutation-based resistance. Cancer Cell *16*, 401–412.

Okram, B., Nagle, A., Adrian, F.J., Lee, C., Ren, P., Wang, X., Sim, T., Xie, Y., Wang, X., Xia, G., et al. (2006). A general strategy for creating "inactive-conformation" abl inhibitors. Chem. Biol. *13*, 779–786.

Pargellis, C., Tong, L., Churchill, L., Cirillo, P.F., Gilmore, T., Graham, A.G., Grob, P.M., Hickey, E.R., Moss, N., Pav, S., et al. (2002). Inhibition of p38 MAP kinase by utilizing a novel allosteric binding site. Nat. Struct. Biol. *9*, 268–272.

Pellicena, P., and Kuriyan, J. (2006). Protein-protein interactions in the allosteric regulation of protein kinases. Curr. Opin. Struct. Biol. *16*, 702–709.

Perera, B.G., and Maly, D.J. (2008). Design, synthesis and characterization of "clickable" 4-anilinoquinazoline kinase inhibitors. Mol. Biosyst. *4*, 542–550.

Quintas-Cardama, A., Kantarjian, H., and Cortes, J. (2007). Flying under the radar: the new wave of BCR-ABL inhibitors. Nat. Rev. Drug Discov. *6*, 834–848.

Schindler, T., Bornmann, W., Pellicena, P., Miller, W.T., Clarkson, B., and Kuriyan, J. (2000). Structural mechanism for STI-571 inhibition of abelson tyrosine kinase. Science *289*, 1938–1942.

Schroeder, G.M., An, Y.M., Cai, Z.W., Chen, X.T., Clark, C., Cornelius, L.A.M., Dai, J., Gullo-Brown, J., Gupta, A., Henley, B., et al. (2009). Discovery of N-(4-(2-Amino-3-chloropyridin-4-yloxy)-3-fluorophenyl)-4-ethoxy-1-(4-fluorophenyl)-2-oxo-1,2-dihydropyridine-3-carboxamide (BMS-777607), a selective and orally efficacious inhibitor of the Met kinase superfamily. J. Med. Chem. *52*, 1251–1254.

Seeliger, M.A., Nagar, B., Frank, F., Cao, X., Henderson, M.N., and Kuriyan, J. (2007). c-Src binds to the cancer drug imatinib with an inactive Abl/c-Kit conformation and a distributed thermodynamic penalty. Structure *15*, 299–311.

Seeliger, M.A., Ranjitkar, P., Kasap, C., Shan, Y., Shaw, D.E., Shah, N.P., Kuriyan, J., and Maly, D.J. (2009). Equally potent inhibition of c-Src and Abl by compounds that recognize inactive kinase conformations. Cancer Res. *69*, 2384–2392.

Simard, J.R., Getlik, M., Grütter, C., Pawar, V., Wulfert, S., Rabiller, M., and Rauh, D. (2009a). Development of a fluorescent-tagged kinase assay system for the detection and characterization of allosteric kinase inhibitors. J. Am. Chem. Soc. *131*, 13286–13296.

Simard, J.R., Kluter, S., Grütter, C., Getlik, M., Rabiller, M., Rode, H.B., and Rauh, D. (2009b). A new screening assay for allosteric inhibitors of cSrc. Nat. Chem. Biol. *5*, 394–396.

Sullivan, J.E., Holdgate, G.A., Campbell, D., Timms, D., Gerhardt, S., Breed, J., Breeze, A.L., Bermingham, A., Pauptit, R.A., Norman, R.A., et al. (2005). Prevention of MKK6-dependent activation by binding to p38alpha MAP kinase. Biochemistry *44*, 16475–16490.

Taylor, S.S., Bubis, J., Toner-Webb, J., Saraswat, L.D., First, E.A., Buechler, J.A., Knighton, D.R., and Sowadski, J. (1988). CAMP-dependent protein kinase: prototype for a family of enzymes. FASEB J. *2*, 2677–2685.

Wan, P.T., Garnett, M.J., Roe, S.M., Lee, S., Niculescu-Duvaz, D., Good, V.M., Jones, C.M., Marshall, C.J., Springer, C.J., Barford, D., and Marais, R. (2004). Mechanism of activation of the RAF-ERK signaling pathway by oncogenic mutations of B-RAF. Cell *116*, 855–867.

Weisberg, E., Manley, P.W., Breitenstein, W., Bruggen, J., Cowan-Jacob, S.W., Ray, A., Huntly, B., Fabbro, D., Fendrich, G., Hall-Meyers, E., et al. (2005). Characterization of AMN107, a selective inhibitor of native and mutant Bcr-Abl. Cancer Cell *7*, 129–141.

Wissing, J., Jansch, L., Nimtz, M., Dieterich, G., Hornberger, R., Keri, G., Wehland, J., and Daub, H. (2007). Proteomics analysis of protein kinases by target class-selective prefractionation and tandem mass spectrometry. Mol. Cell. Proteomics *6*, 537–547.

Wong, L., Jennings, P.A., and Adams, J.A. (2004). Communication pathways between the nucleotide pocket and distal regulatory sites in protein kinases. Acc. Chem. Res. *37*, 304–311.

